SPECTROPHOTOMETRY OF COMET HARTLEY-GOOD (1985l)

B. S. RAUTELA

Uttar Pradesh State Observatory, Manora Peak, Nainital, India

P. S. GORAYA

Department of Astronomy and Space Sciences, Punjabi University, Patiala, India

B. B. SANWAL

Uttar Pradesh State Observatory, Manora Peak, Nainital, India

and

S. K. GUPTA

Uttar Pradesh State Observatory, Monara Peak, Nainital, India

(Received 3 January, 1989)

Abstract. We present spectrophotometric studies of comet Hartley-Good (1985l) in the spectral region $\lambda\lambda$3200-7000 Å. The emission features of molecules CN, CH, C_2, and C_3 are observed. The variation of the emission strength of different species has been studied as a function of heliocentric distance. The abundances (N) and production rates (Q) of the molecules are also estimated.

1. Introduction

Comet Hartley-Good (1985l) was discovered on a single objective-prism plate at the back of the 1.2 m Schmidt telescope of U.K. At the time of discovery the total integrated magnitude (m_1) was ~12 and the comet had developed a tail (Hartley and Good, 1985). Later estimates have appeared in various IAU circulars (Cir. Nos. 4109, 4113, 4122, 4130, 4139, 4156). Some astrometric observations have also been reported in the IAU circulars (Cir. Nos. 4109, 4113, 4130).

Goraya and Rautela (1985) and Goraya *et al.* (1986b) were the first observers to report different emission features observed by them in comet Hartley-Good. They observed the emissions due to CN, CH, C_2, and C_3 molecules in it. So far, no such other study has been reported in literature. In the present investigation, we present spectrophotometric observations and detailed analysis of comet Hartley-Good.

2. Observations

The observations were made on six nights during November, 1985 when the comet was sufficiently bright for the limit of our instrument (cf. Table I).

Earth, Moon, and Planets **44**: 233-242, 1989.

TABLE I

Summary of the Observations

Date (UT) 1985	Geocentric[a] distance (Δ) AU	Heliocentric[a] distance (r) AU	Predicted[a] m_1
Nov. 22.58	0.97	0.77	6.19
Nov. 23.56	0.98	0.76	6.17
Nov. 24.57	0.99	0.75	6.16
Nov. 25.54	1.00	0.74	6.14
Nov. 26.55	1.00	0.74	6.13
Nov. 27.54	1.01	0.73	6.12

Reference:
[a]Marsden (1985).

Observations were made with Hilger and Watts spectrum scanner (Goraya *et al.*, 1982, 1984) at the Cassegrain focus ($f/13$) of the 104 cm reflector of the Nainital Observatory. The spectrum scanner gives a dispersion of 70 Å mm^{-1} in the first order. We used a circular diaphragm of 3 mm which corresponds to 45 arc sec as projected on the sky to allow the whole light from the head of the comet to enter the instrument. An exit slit of 0.7 mm allowing 50 Å of the spectrum to fall on the photomultiplier was used. The photomultiplier EMI 9658 B was cooled to (−20 °C) and standard d.c. techniques for detecting and recording the signal were followed (Goraya *et al.*, 1982, 1984). At least three spectral scans of the comet were obtained every night and were reduced to instrumental magnitudes individually at a step of 25 Å. The means of the instrumental magnitudes were adopted. We also obtained scans of the neighboring sky before and after each scan of the comet to eliminate the contribution of the background sky.

Along with comet Hartley-Good, the standard star ξ^2 Cet was observed many times during each night to evaluate atmospheric extinction and to convert mean instrumental magnitudes of the comet to standard magnitudes, which thus corresponds to the recent calibration of ξ^2 Cet given by Taylor (1984). Finally, the standard monochromatic magnitudes (m_λ) of the comet were converted to fluxes (F_ν) by use of the relation

$$\log F_\nu = -19.447 - 0.4 m_\lambda \, . \qquad (1)$$

3. Strength of Emission Features

The final spectra of comet Hartley-Good are displayed in Figure 1. The positions of different emission features are indicated by vertical arrows pointing downwards. There are no large gradual variations in the strength of emission bands. The continuum level has also not changed appreciably during the observing period. Figure 1 clearly shows the emission due to CN(1–0) λ3580 Å, CN(0–0) λ3880 Å, CN(0–1) λ4200 Å, CH(0–0) + C_3 λ4050 Å, CH(0–0) + C_2(2–0)

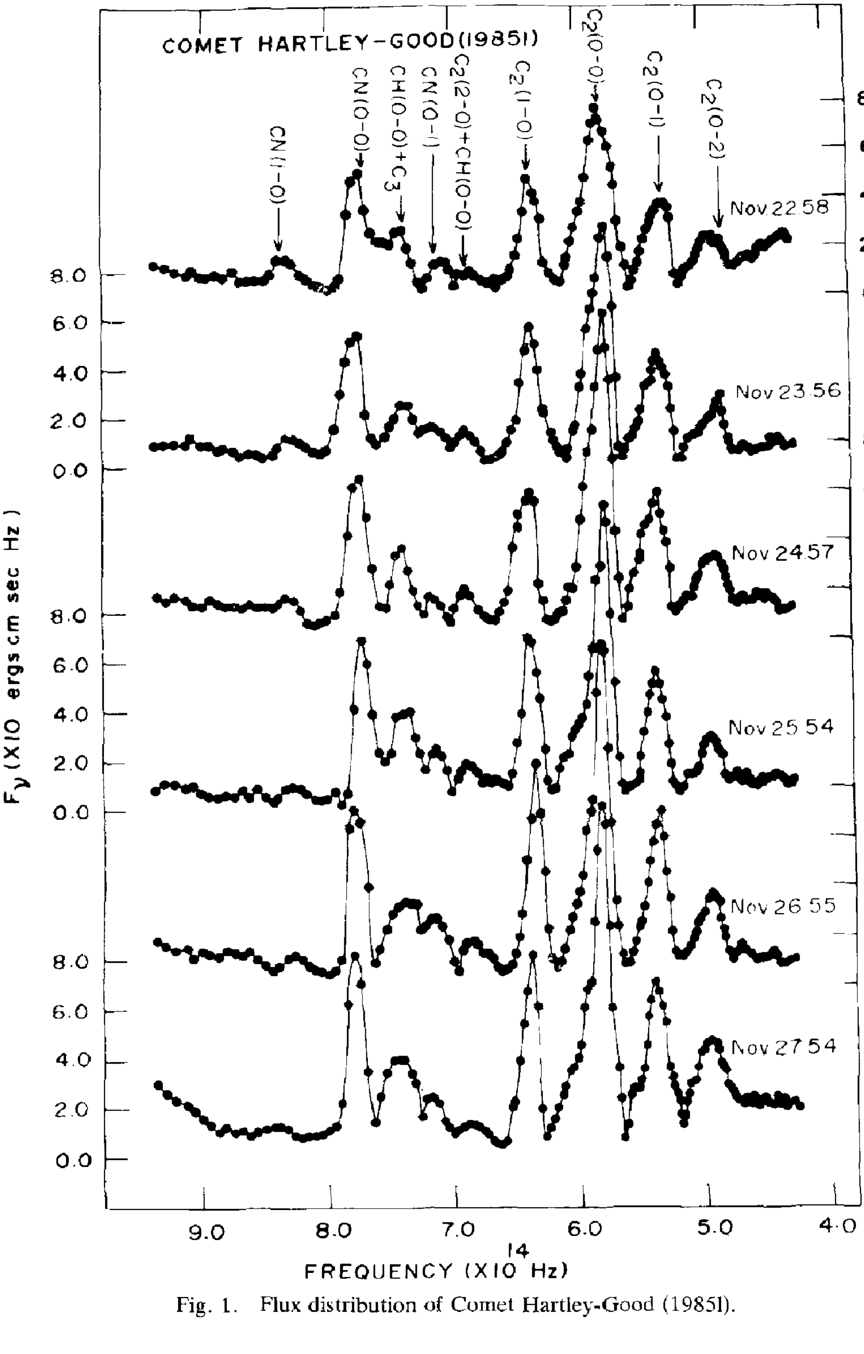

Fig. 1. Flux distribution of Comet Hartley-Good (1985l).

λ4350 Å, C_2(1–0) λ4700 Å, C_2(0–0) λ5160 Å, C_2(0–1) λ5640 Å and C_2(0–2) λ6190 Å molecules. To derive the emission strength of different species, we measure the total area under the emission bands relative to the continuum level. The continuum in the spectrum was drawn by selecting wavelength regions free

TABLE II

Fluxes of emission bands relative to $C_2(0-0)$

Date (UT) 1985	Apparent flux (F) in the $C_2(0-0)$ band (ergs cm^{-2} sec^{-1}) $\times 10^{-10}$	$F/F[C_2(0-0)]$									Luminosity (L) in the $C_2(0-0)$ band (ergs sec^{-1}) $\times 10^{17}$
		CN(1–0)	CN(0–0)	CH(0–0) + C_3	CN(0–1)	$C_2(2-0)$ + CH(0–0)	$C_2(1-0)$	$C_2(0-1)$	$C_2(0-1)$	$C_2(0-2)$	
Nov. 22.58	1.944	0.113	0.497	0.228	0.085	0.042	0.386	1.000	0.391	0.199	5.144
Nov. 23.56	2.022	0.071	0.471	0.208	0.119	0.066	0.485	1.000	0.425	0.186	5.460
Nov. 24.57	2.650	0.044	0.392	0.169	0.033	0.057	0.390	1.000	0.400	0.203	7.304
Nov. 25.54	2.160	0.046	0.471	0.310	0.103	0.059	0.440	1.000	0.343	0.174	6.075
Nov. 26.55	2.406	0.044	0.415	0.288	0.159	0.071	0.459	1.000	0.411	0.226	6.834
Nov. 27.54	2.746	0.021	0.412	0.295	0.082	0.046	0.380	1.000	0.433	0.262	7.878

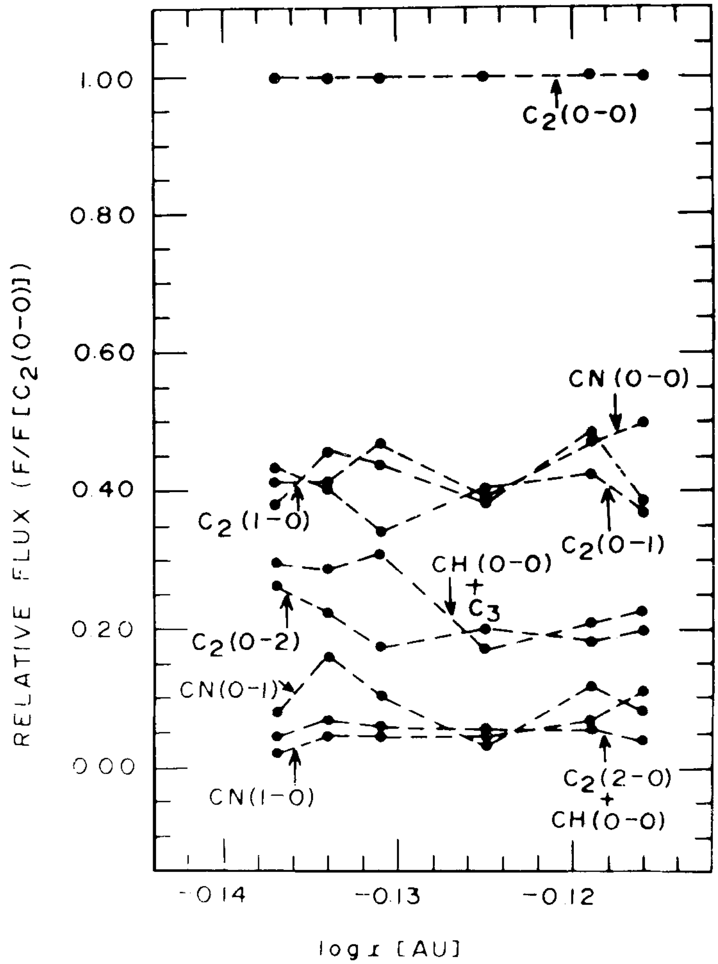

Fig. 2. Variation of the relative flux of emission bands as a function of heliocentric distance.

of emission lines. The area of the emission bands was converted into flux. The total apparent fluxes in different emissions bands relative to C_2(0–0) band flux are given in Table II. The total luminosity in the C_2(0–0) band is given to the last column of Table II. The relative fluxes display fluctuations in their strength (cf. Figure 2). This implies that the brightness of the comet display night-to-night variation. Such variations may be due to some intrinsic causes taking place inside the comet.

4. Number of CN and C_2 Molecules

The total number of molecules (N) of CN and C_2 contained in a cylinder of diameter 45 arc sec in the line of sight and extending through the head of the

TABLE III

Number of CN and C_2 molecules

Band	f	p	$\rho(\nu, r)$ erg cm^{-3}	log N					
				Nov. 22.58	Nov. 23.56	Nov. 24.54	Nov. 25.54	Nov. 26.55	Nov. 27.54
CN(0_0)	0.0342[a]	0.9200[b]	4.214×10^{-20} r^{-2} [b]	29.151	29.148	29.184	29.172	29.162	29.214
CN(0–1)	0.0024[a]	0.8108[b]	6.910×10^{-20} r^{-2} [b]	29.381	29.544	29.106	29.507	29.739	29.505
C_2(1–0)	0.0089[b]	0.2409[b]	7.140×10^{-20} r^{-2} [b]	29.979	30.099	30.119	30.080	30.143	30.117
C_2(0–0)	0.0239[a]	0.7335[b]	6.445×10^{-20} r^{-2} [b]	29.525	29.545	29.660	29.568	29.614	29.668
C_2(0–1)	0.0071[b]	0.2142[b]	8.390×10^{-20} r^{-2} [b]	30.064	30.121	30.209	30.050	30.175	30.253

References:
[a] Lambert (1978).
[b] Goraya *et al.* (1986a).

comet can be derived from the total energy emitted in the CN and C_2 emission bands. A gross estimate of the total number of molecules of different species is made by using the well known relation (cf. O'Dell and Osterbrock, 1962) and recently adopted by many authors (Sivaraman *et al.*, 1979, Goraya *et al.*, 1982, 1984, 1986a):

$$N = L \frac{m_e}{\pi e^2 f p \rho(\nu, r)}, \tag{2}$$

where

L = luminosity of the respective band;
m_e = mass of an electron;
e = charge of an electron;
p = the vibrational transition probability;
f = the oscillator strength; and
$\rho(\nu, r)$ = the solar radiation density at frequency ν at a heliocentric distance r.

The values of f, p and $\rho(\nu, r)$ used in our calculations are adopted from Lambert (1978) and Goraya *et al.* (1986a) and are listed in Table III alongwith the total number of molecules estimated by us.

5. Production Rates of CN, C_3, and C_2 Molecules

Production rates can be derived from the total luminosity of the emission band. For making an estimate of the production rates of different molecules we assume that the excitation processes responsible in the coma of the comet are induced by solar radiation. Collisions within the coma and excitation by solar wind particles are neglected. For resonance scattering and fluorescence, the luminosity, L, is related to the total number of atoms or molecules, N, and to the emission rate factor, g, by the relation (cf. Barth, 1969)

$$L = gN. \tag{3}$$

In terms of life time, τ, one has

$$Q = \frac{N}{\tau} = \frac{4\pi\Delta^2 F}{g\tau}, \tag{4}$$

where

Δ = the comet-Earth distance;
F = the observed flux from the comet;
τ = the life-time of the scattering species; and
g = the probability that a solar photon will be resonantly scattered or produced by resonance fluorescence.

The values of g and τ used in our calculations are given in Table IV along with

TABLE IV

Life times and emission rate factors of CN, C_2, and C_3 species

Species	Emission rate factor[a] (g) photon/sec/mol	Life time[b] (τ) sec	Product ($g\tau$)
CN	7.42×10^{-2}	14.8×10^4	1.098×10^4
C_2	4.38×10^{-2}	6.6×10^4	2.891×10^3
C_3	4.40×10^{-1}	4.0×10^4	1.760×10^4

References:
[a] Newburn *et al.* (1978).
[b] A'Hearn and Cowan (1975).

their sources. The production rates of CN, C_2 and C_3 molecules are listed in Table V. Actually, the life-times are never observed directly. They are derived by dividing the observed scale length, s, by the assumed mean expansion velocity of the molecules. The life-time, τ, is principally determined by photodestruction process, the product $g\tau$ is independent of the heliocentric distance, (Feldman *et al.*, 1974) and can be conveniently evaluated at IAU. The g-factors and life

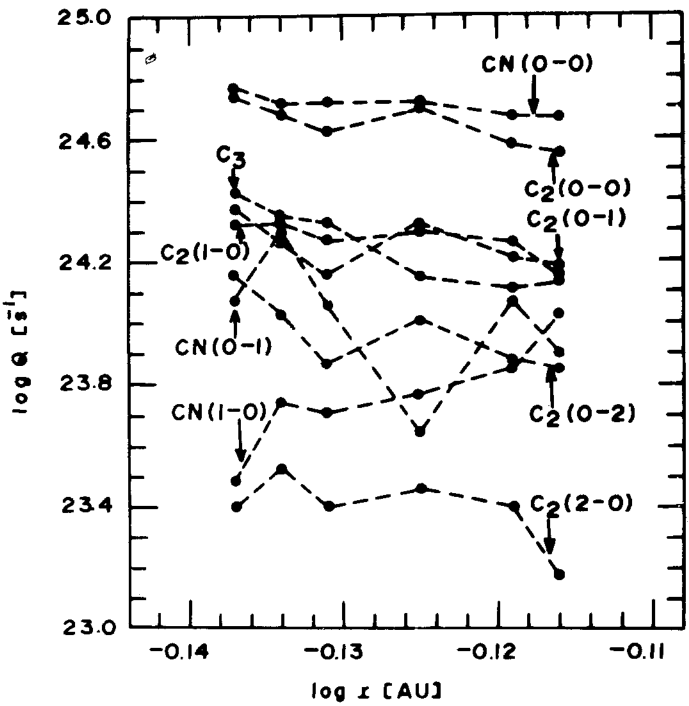

Fig. 3. Variation of production rates of emission bands as a function of heliocentric distance.

TABLE V

Production rates of CN, C_2 and C_3 molecules

Date (UT) 1985	log r (AU)	log Q CN(1–0)	log Q CN(0–0)	log Q CN(0–1)	log Q C_3	log Q				
						C_2(2–0)	C_2(1–0)	C_2(0–0)	C_2(0–1)	C_2(0–2)
Nov. 22.58	−0.116	24.028	24.670	23.905	24.128	23.179	24.140	24.553	24.146	23.851
Nov. 23.56	−0.119	23.852	24.673	24.074	24.112	23.401	24.265	24.579	24.208	23.849
Nov. 24.57	−0.125	23.767	24.720	23.647	24.149	23.459	24.297	24.706	24.308	24.013
Nov. 25.54	−0.131	23.712	24.719	24.060	24.333	23.398	24.269	24.626	24.160	23.866
Nov. 26.55	−0.134	23.741	24.715	24.298	24.351	23.526	24.338	24.677	24.291	24.031
Nov. 27.54	−0.137	23.484	24.773	24.070	24.424	23.400	24.318	24.739	24.375	24.157

times may be uncertain by as much as ± 50% producing the same order of uncertainty in the production rates.

A plot of the variation of production rates of different species with heliocentric distance is shown in Figure 3. The production rates display night-to-night fluctuations but the general tendency is the increase in production rates with decreasing heliocentric distance.

References

A'Hearn, M. F. and Cowan, J. J.: 1975, *Astron. J.* **80**, 852.

Barth, C. A.: 1969, *Appl. Optics* **8**, 1295.

Feldman, P. D., Takacs, P. Z., and Fastie, W. G.: 1974, *Science* **185**, 705.

Goraya, P. S., Sinha, B. K., Chaubey, U. S., and Sanwal, B. B.: 1982, *The Moon and the Planets* **26**, 3.

Goraya, P. S., Rautela, B. S., and Sanwal, B. B.: 1984, *Earth, Moon, and Planets* **30**, 63.

Goraya, P. S. and Rautela, B. S.: 1985, *IAU Circ.* No. 4150.

Goraya, P. S., Rautela, B. S., and Sanwal, B. B.: 1986a, *Earth, Moon, and Planets* **34**, 77.

Goraya, P. S., Rautela, B. S., and Sanwal, B. B.: 1986b, *IAU Circ.* No. 4171.

Hartley, M. and Good, A.: 1985, *IAU Circ.* No. 4107.

Lambert, D.: 1978, *Mon. Not. Roy. Astron. Soc.* **182**, 249.

Marsden, B. G.: 1985, *IAU Circ.* No. 4130.

Newburn, R. L., J. R., and Johnson, T. V.: 1978, *Icarus* **35**, 360.

O'Dell, C. R. and Osterbrock, D. E.: 1962, *Astrophys. J.* **136**, 559.

Sivaraman, K. R., Babu, G. S. D., Bappu, M. K. V., and Parthasarathy, M.: 1979, *Mon. Not. Roy. Astron. Soc.* **189**, 897.

Taylor, B. J.: 1984, *Astrophys. J. Suppl.* **54**, 259.